American Scientific Research Journal for Engineering, Technology, and Sciences (ASRJETS)
ISSN (Print) 2313-4410, ISSN (Online) 2313-4402

http://asrjetsjournal.org/

Predictions of the Electric Field Emissions around Power Transmission Lines by Using Artificial Neural Network Methods

H. Feza Carlak[a*], Şükrü Özen[b], Süleyman Bilgin[c]

[a,b,c]*Deparments of Electrical and Electronics Engineering, Akdeniz University, Antalya 07058, Turkey*

[a]*Email: fezacarlak@akdeniz.edu.tr*

[b]*Email: sukruozen@akdeniz.edu.tr*

[c]*Email: suleymanbilgin@akdeniz.edu.tr*

Abstract

In this study, Artificial Neural Network (ANN) Algorithms are used to estimate the electric field that occurred around the power transmission lines as an alternative approach. Firstly, electric field levels around the high voltage power transmission lines are measured, and then analytically calculated. Moreover, the field levels that occurred around these power lines have been predicted by using multilayer perceptron artificial neural network, radial basis function, and generalized regression neural network models. In the paper, 154 kV typical power transmission line used in Turkey are studied. Electric field levels occurred around the power transmission lines have been predicted with ANN models with high accuracy, particularly MLPNN algorithm predicted the electric field intensity with very high precision.

Keywords: Power Transmission Lines; Electric Field Emissions; Artificial Neural Network Algorithms.

1. Introduction

The electrical power transmission and distributions systems induce an extremely low frequency electric and magnetic fields. Since 1980, power frequency electric and magnetic fields have been taking an important attention due to concerns that exposure of such fields might cause undesired health effects [1,2,3,4,25].

---

* Corresponding author.

Growing interest in epidemiological studies aims at establishing possible links between an exposures of residential or occupational to power frequency fields and the onset of a number of diseases, including cancer and leukemia have been witnessed in the last few years [5,6,7]. Past epidemiologic studies have been criticized for some methodological shortcomings, especially regarding the way such exposure were evaluated [8,9,26].

Table 1: ICNIRP Exposure Limits for Electrical Workers (at 50 Hz) [27]

	General Public	Occupational
Electrical Field Strength (E)	5 kV/m	10 kV/m
Magnetic Flux Density (B)	200 μT	1000 μT

One of the recent study showed that the leukemia risk for children has been increasing and also due to residential exposures of ELF-EMF, the cancer risk of adult people has been observed in some of the studies. The leukemia risk for adult rises dramatically around the power transmission lines. The people who live in the 50 m vicinity of the transmission line have 33 % higher cancer risk to the people who live in the field of 50 m to 100 m [10,11,12,13].

In the studies of the high voltage power line, researchers have focused more on the magnetic field exposure in the literature. However, outdoor exposure of the electric fields around the power transmission lines can have harmful effects on human health and should be taken into account for the human health. In particular, the electric field exposure for workers of power lines and public living in the vicinity of power lines is critical. Furthermore, these electric field intensity values will generate an important database for studies of the human health researchers.

A lower bound on neural network discrimination of 1 mV m-1 has been suggested, but based on current evidence, threshold values around 10–100 mV m-1 seem to be more likely. With regard to indirect effects, the surface electric charge induced by electric fields can be perceived, and it can result in painful micro shocks when touching a conductive object. Exposure to power-frequency electric fields causes well-defined biological responses, ranging from perception to annoyance, through surface electric charge effects [14]. These responses depend on the field strength, the ambient environmental conditions and individual sensitivity. The thresholds for direct perception by 10% of volunteers varied between 2 and 20 kV m-1, while 5% found 15–20 kV m-1 annoying. The spark discharge from a person to ground is found to be painful by 7 % of volunteers in a field of 5 kV m-1. Thresholds for the discharge from a charged object through a grounded person depend on the size of the object and therefore require specific assessment [15]. The threshold is likely to be constant over a frequency range between a few hertz and a few kilohertz. Furthermore, sensitivity to electrical stimulation of the CNS seems likely to be associated with a family history of seizure and the use of tricyclic antidepressants, neuroleptic agents and other drugs that lower the seizure threshold. The function of the retina, which is a part of the CNS, can be affected by exposure to much weaker ELF magnetic fields than those that cause direct nerve stimulation.

At residential life, childhood cancers and occupational cancers as breast & brain cancer and leukemia have been dramatically increasing due to the harmful effects of power frequency electromagnetic fields on human health.

There are also other undesired detrimental effects of the electromagnetic field exposure, i.e., the increase of the risk of getting miscarriage [16] neurodegenerative diseases such as amyotrophic lateral sclerosis and Alzheimer's disease [17].

This study will shed light on the comparison of traditional methods with the method of artificial neural networks to be able to estimate the electric fields on the power lines. For this goal, electric field variations around the typical power lines used in Turkey are investigated. A number of analytic and numerical methods for calculation of electric field around the electric power transmission and distribution lines are implemented. Artificial neural networks have been widely used in recent years at various research applications such as predictions, pattern recognitions, classifications, medical applications, automatic control and signal processing. Many interesting applications have been presented in power systems, such as load forecasting, fault classifications and locations in transmission lines, voltage stability analysis and power systems economics. The Multi-Layer Perceptron (MLP) which is trained by the back propagation algorithm is the most popular artificial neural networks in engineering problems.

This paper presents predicted electric field levels occurred around typical power transmission lines used in Turkey by implementing Multilayer Perceptron Neural Networks (MLPNN) and Radial Basis Functions model algorithms as an alternative approach.

2. Theoretical Calculation of Electric Fields

The calculation of power frequency electric fields around the power transmission lines requires separate evaluations due to the quasi-static field approach. In this study, charge simulation methods is used for the electric field calculation. In this study, Charge Simulation Method (CSM) was implemented to obtain the electric fields around the high voltage transmission lines [18]. The electric potential Vi at any point whether in the insulating region or at the surface of a conductor can be calculated by the summation of the potential contribution of all the individual simulation charges (equation 1).

$$V_i = \sum_{j=1}^{n} P_{ij} \cdot q_i \qquad (1)$$

where, P_{ij} is the potential coefficient related to the potential of the jth charge at the ith point, q_i is the simulation charges, n is the charge number. The electric field intensity is calculated using the following equation.

$$\vec{E} = -\nabla V \ \text{(V/m)} \qquad (2)$$

3. Electric Field Measurement

Residential electric fields radiated from typical high voltage power lines used in Turkey were measured by using CA42 LF field meter, the Chauvin Arnoux. Electric field measurements were taken at 1m height from the

ground level, physical characteristics of the 154 kV power lines is shown in Figure 1. and Table 2. Since 154 kV power

lines pass through the center of population in Turkey, measurements were acquired particularly for this voltage level.

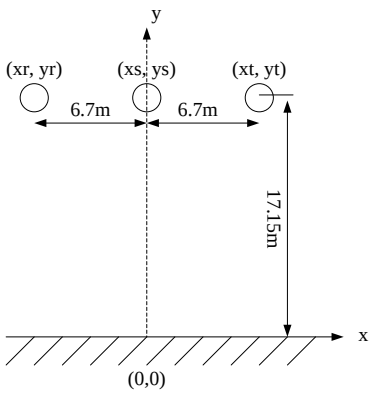

Figure 1: Cross-section of 154 kV energy power transmission lines.

4. Artificial Neural Network Algorithms

The electric fields are determined by the prediction methods and measurements. For the long term prediction of this field, load characteristics of the lines are considered for a year period. In the literature, there are limited number of studies implemented with the electric fields for exposure analysis using Multilayer artificial neural network algorithms. These studies present an alternative approaches. Generally, researchers focused on the magnetic field exposure, but electric and magnetic field components can be induced to the human body with together. Electric field variations around the lines are determined by using Charge Simulation Method (CSM). A computer program is developed to simulate electric field variation around the power transmission lines.

4.1. Multilayer perceptron neural networks (MLPNN)

MLPNN is used as one of the most common Neural Network Algorithms. MLPNN may include two or more layers as shown in Figure 3. Input layer has neurons which are equal to the number of selected specific features and output layer determine the desired output classes which decide the number of the neurons in the output layer. The hidden layers which are between input and output layers may be used for optimizing of MLPNN especially for nonlinear systems. It is typical using just one hidden layer with a try and-error based number of neurons. The most common method to find the optimal number of neurons and hidden layers is by try-and-error [19]. An MLPNN occurs perceptron model based on Rosenblatt model in the 1950's [20] shown in Figure 2.For one perceptron, the MLPNN is shown as,

$$x = \sum_{i=1}^{R} w_i p_i + b \qquad (5)$$

where; *R* is the number of inputs and their weights, p_i are the input values of a perceptron and w_i are weights for each inputs, *x* is the summation of a perceptron. The summation of the perceptron is scaled with tangent sigmoid activation function in the hidden layers and linear transfer function in the output layer. The output *y* of a perceptron for Tangent Sigmoid function in the hidden layers is denoted as;

$$y = f(x) = \frac{e^{x} - e^{-x}}{e^{x} + e^{-x}} \quad (6)$$

Linear transfer function $y=f(x)=x$ can be calculated at the once perceptron in the output layer. The structure of MLPNN model is shown in figure 3 $\{(p_n, t_n)\}$ are training patterns, *n* is the pattern number, the R and Q are the dimensions of the input vector p_n and desired output vector t_n respectively, vector y_n is the network output of the *n-th* pattern. For the *I-th* hidden unit, the net input $net_n(I)$ and the output activation $O_n(I)$ for the *n-th* training pattern are;

$$net_n(i) = \sum_{j=1}^{R+1} \omega(i,j).p_n(j), \quad 1 \le i \le N \quad (7)$$

$$O_n(i) = f\left(net_n(i)\right) \quad (8)$$

where $\omega(I,j)$ shows the weight connecting the *j*-th input unit to the *I*-th hidden unit. The *k*-th output for the *n*-th training pattern is y_{nk} is given as the following equation,

$$y_{nk} = \sum_{j=0}^{R+1} \omega_{jo}(k,j) \cdot p_n(j) + \sum_{i=1}^{Nh} \omega_{ho}(k,i) \cdot O_n(i), \quad 1 \le k \le Q \quad (9)$$

where $\omega_{io}(k,j)$ denotes the output weight connecting the *j*-th input unit to the *k*-th output unit and $w_{ho}(k,I)$ denotes the output weight connecting the *I*-th hidden unit to the *k*-th output unit. The mapping error for the *n*-th pattern is given by,

$$E_n = \sum_{k=1}^{Q} [t_{nk} - y_{nk}]^2 \quad (10)$$

where t_{nk} denotes the *k*-th element of the *n*-th desired output vector. Training a neural network in batch mode, the mapping error for the *k*-th output unit is formulized by,

$$E(k) = \frac{1}{N_h} \sum_{n=1}^{N_h} [t_{nk} - y_{nk}]^2 \quad (11)$$

The overall performance of an MLPNN, measured as the mean square error (MSE), can be given as

$$E = \sum_{k=1}^{Q} E(k) \quad (12)$$

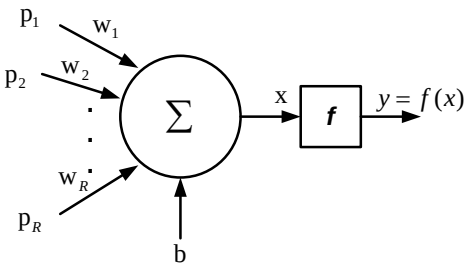

Figure 2: The structure of one perceptron.

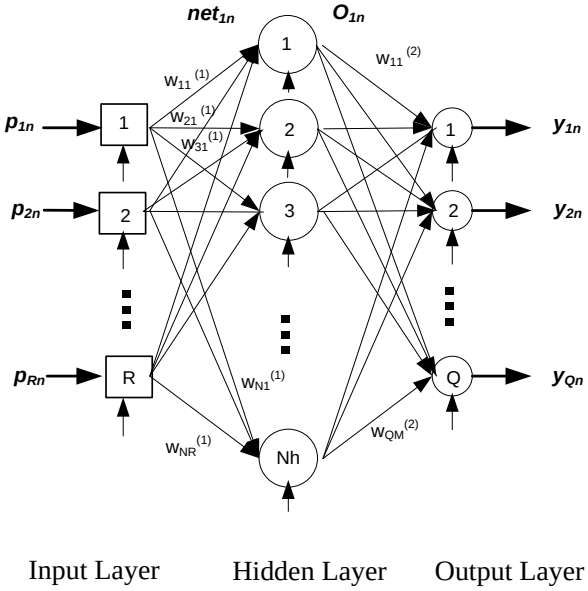

Figure 3: The Structure of a general MLPNN model

4.2. Radial basis function (RBF)

References The RBFNN is an alternative method to MLPNN and requires less computation time than MLPNN for network training. RBFNN is comprised of one input layer, one kernel (hidden), and one output layer. The structure of the RBF model is denoted in figure 4. The input variables are assigned to the nodes within the input layer and connected to the hidden layer without weights. The transfer functions in the hidden nodes are RBF that means symmetrical function centered upon a given mean value in a space. The parameters are optimized during the network training in RBFNN. When the training vectors are measured up to presumed level, linear combinations of RBFs can be found at the training vectors. The method of fitting RBF's to data is closely related to the distance weighted regression, for function approximation.

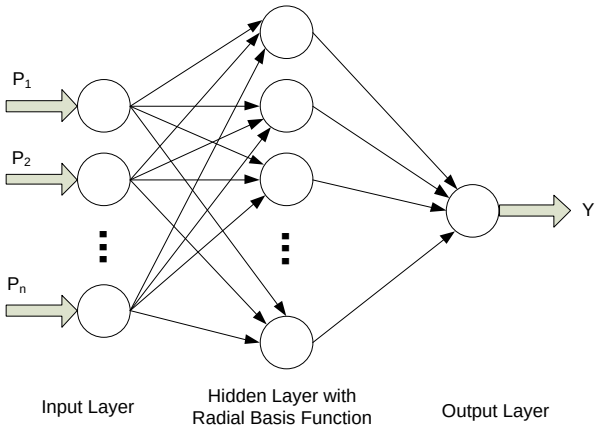

Figure 4: The Structure of a general RBFNN model

The RBFNN is formulated as following expression;

$$y = \omega_0 + \sum_{i=1}^{n_h} \omega_i \, f\left(\left\|\mathbf{X} - \mathbf{c_i}\right\|\right) \qquad (13)$$

Where, f are the radial basis functions, ω_i are the output layer weights, ω_0 is the output offset, **X** are the inputs of the network as $\mathbf{X}=[x_1, \ldots, x_n]'$, $\mathbf{c_i}$ are the centers associated with the basis functions, n_h is the number of basis functions in the network, and $\|\cdot\|$ denotes the Euclidean norm. It is denoted as;

$$\|\mathbf{X}\| = \left(\sum_{i=1}^{n} x_i^2\right)^{\frac{1}{2}} \qquad (14)$$

The nonlinear basis function can be formulated by Gaussian function;

$$f\left(x\right) = e^{-\frac{(x-c)^2}{r^2}} \qquad (15)$$

where, c is the center of the basis function which has Radius r.

RBFNN can be trained with the following procedure, at first, the centers $\mathbf{c_i}$ of the hidden neuron activation functions can be initialized using clustering algorithm which is the unsupervised training. Then, the parameters in RBFNN are updated by gradient-based optimization techniques. Training data set includes $Q=\{q_1,q_2,\ldots,q_n\}$ and the each element of this set is defined as $q_k = (p_k,t_{dk})$ where $p_k=(p_{1k}, p_{2k}, \ldots, p_{Rk})$ and t_{dk} is the desired response. The aim of this technique is minimizing the E parameters in the following equation;

$$E = \frac{1}{2}\sum_{k=0}^{N}(t_{dk} - t_k)^2 \tag{16}$$

where t_k is the output of the network related to input vector p_k.

$$\omega_{i,j}(l+1) = \omega_{i,j}(l) - \eta_\omega \frac{\partial E}{\partial \omega_{i,j}} \tag{17}$$

$$\omega_{i,j}(l+1) = \omega_{i,j}(l) - \eta_\omega \sum_{k=1}^{N} \frac{(t_{dk} - t_k)}{\sum_{i=1}^{s} v_{ik}} \frac{(p_{jk} - \omega_{i,j})}{b_i^2} v_{ik} (\omega_i - t_k) \tag{18}$$

and

$$b_i(l+1) = b_i(l) - \eta_b \frac{\partial E}{\partial b_i} \tag{19}$$

$$b_i(l+1) = b_i(l) - \eta_b \frac{(t_{dk} - t_k)}{\sum_{i=1}^{n} v_{ik}} v_{ik} \sum_{k=1}^{N} \frac{(p_{jk} - \omega_{i,j})^2}{b_i^3} (\omega_i - t_k) \tag{20}$$

and

$$\omega_i(l+1) = \omega_i(l) - \eta_\omega \frac{\partial E}{\partial \omega_i} \tag{21}$$

$$\omega_i(l+1) = \omega_i(l) + \eta_\gamma \frac{(t_{dk} - t_k)}{\sum_{i=1}^{s} v_{ik}} v_{ik} \tag{22}$$

where

$$v_{ik} = e^{-\sum_{j=1}^{R} \frac{(p_{jk} - \omega_{i,j})^2}{2b_i^2}} \tag{23}$$

and η_ω, η_b, η_γ are the update rates for updating the parameters ω_{ij}, b_i and ω_i respectively. The gradient descent algorithm based on the (7), (9), (11) training of the RBFNN is implemented in MATLAB.

4.3. Generalized Regression Neural Networks (GRNN)

The GRNN comprises of four layers; input layer, pattern layer, summation layer and output layer (see Fig. 5). This regression tool consists of a dynamic network structure. The GRNN model has X input values vector and Y output values vector. Thus, x and y are measured values of X and Y respectively, and $\hat{f}(x, y)$ is the joint continuous probability density function of X and Y. The joint probability density in GRNN can be expressed as;

$$\hat{f}(x,y)=\frac{1}{(2\pi)^{(d+1)/2}}\times\frac{1}{n}\sum\left[\exp\left(\frac{(x-x_i)^T(x-x_i)}{2\sigma^2}\right)\exp\left(\frac{(y-y_i)^2}{2\sigma^2}\right)\right] \quad (24)$$

Where n is the sample observations, σ is the spread parameter, x_i is the i-*th* training vector, vector y_i is the corresponding value. The regression of Y on x can be formulated as;

$$E[Y\mid x]=\frac{\int_{-\infty}^{\infty}Y.f(x,Y)dY}{\int_{-\infty}^{\infty}f(x,Y)dY} \quad (25)$$

and,

$$\hat{y}(x)=E[Y|x]=\frac{\sum_{i=1}^{n}\left[y_i\exp(\frac{-d_i^2}{2\sigma^2})\right]}{\sum_{i=1}^{n}\exp(\frac{-d_i^2}{2\sigma^2})} \quad (26)$$

Where d_i is the distance between the input vector and the *i-th* training vector, and is denoted as,

$$d_i^2=(x-x_i)^T(x-x_i) \quad (27)$$

The estimate $\hat{y}(x)$ is a weighted average of all observed y_i values.

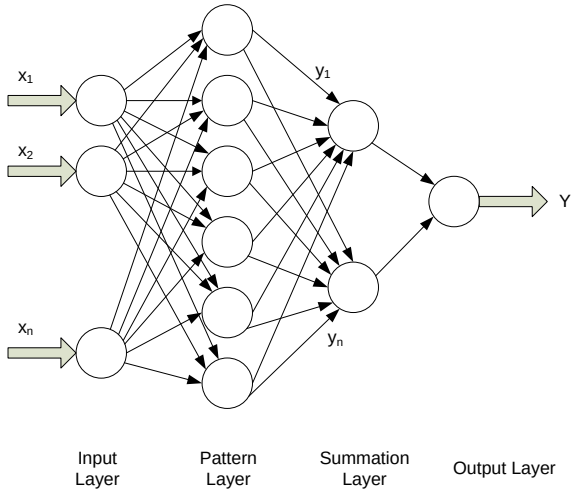

Figure 5: The structure of GRNN

5. Results & Discussion

In this study, three ANN method results are compared for calculating the electric field. These methods are Multilayer Perceptron Neural Networks (MLPNN), Radial Basis Function (RBF) and Generalized Radial Basis

Neural Networks (GRNN). The MLPNN trained by the back propagation algorithm is the most popular method in engineering problems [19,22]. The training dataset is shown in Table 2.

The method of MLPNN is firstly implemented for calculation. In order to obtain the Neural Network performance, following steps have been implemented:

1. The normalization of input and output datasets with maximum minimum mapping ranging between -1 and 1. Input values are selected as horizontal and vertical distance values. The output values are selected as measured electric field values. So, the ANN structure has two input values and one output values.

2. The database is divided into 60 % train, 15 % validation and 25 % test datasets randomly.

3. The determination of target values according to maximum minimum mapping.

4. The MLPNN structure occurs from an input layer having two neurons, three hidden layers having two, three, two neurons with tangent sigmoid transfer function in each hidden layers respectively and an output layer having one neuron with linear transfer function.

5. The structure is determined as experimental and the selected structure has the highest scores of achievement.

6. This structure is trained using Levenberg-Marquardt algorithm that determines the most optimum values between other back propagation training algorithms used as experimental comparison [23].

7. Test accuracy of Training Simulation is determined according to mse (Mean Squared Error) scores.

8. Test accuracy of Testing Simulation is also determined by mse scores.

9. The achievement is compared with other methods as relative errors and mse scores.

In the RBF analysis, database is selected as 75% for training and 25% for test. So, it has an input layer with two neurons, one hidden layer including radial basis functions and one output having one neuron. Input data is directly connected to the hidden layer without having weighted in contrast to the MLPNN model [23,24]. The neuron in the hidden layer is delicate for data points near its center. This sensitivity is adjusted by selection of the spread factor, where a smaller spread factor states more precision. The spread factor is chosen as 0.6 by trial and error.

In the GRNN analysis, database is selected as 75% for training and 25% for test similar to RBF structure. It has an input layer with two neurons, one pattern layer including radial basis functions, a summation layer and one output having one neuron. Spread factor that is only adjustable parameter in GRNN structure is selected as 0.5 experimentally in this study. The spread parameter is the distance an input vector from the weight vector of a neuron.

Table 2: Training Dataset

X(m)	Y(m)									
	0,2		**0,5**		**1**		**1,5**		**2**	
	Ecal	Emeas.	Ecal	Emeas.	Ecal	Emeas.	Ecal	Emeas.	Ecal	Emeas.
0	1,124	1,164	1,16	1,18	1,224	1,26	1,294	1,3	1,369	1,4
3	1,101	1,13	1,136	1,1	1,198	1,22	1,265	1,255	1,338	1,37
6	1,036	1,1	1,068	1,032	1,123	1,16	1,183	1,14	1,248	1,3
9	0,9396	0,95	0,9659	0,93	1,012	0,98	1,062	1,1	1,115	1,119
12	0,8261	0,798	0,8466	0,81	0,8826	0,905	0,9206	0,928	0,961	0,98
15	0,7106	0,735	0,7259	0,75	0,7524	0,742	0,7801	0,81	0,8092	0,842
18	0,6037	0,59	0,6148	0,59	0,6337	0,64	0,6533	0,67	0,6736	0,68
21	0,5106	0,53	0,5185	0,535	0,5318	0,521	0,5455	0,531	0,5595	0,56
24	0,4323	0,42	0,4379	0,45	0,4473	0,448	0,4569	0,44	0,4666	0,464
27	0,3675	0,358	0,3716	0,35	0,3783	0,365	0,3851	0,4	0,3919	0,4
30	0,3145	0,32	0,3174	0,3	0,3223	0,31	0,3272	0,332	0,332	0,321
33	0,271	0,28	0,2731	0,26	0,2767	0,276	0,2803	0,283	0,2838	0,29
36	0,2352	0,228	0,2368	0,24	0,2395	0,235	0,2421	0,246	0,2447	0,254
39	0,2056	0,199	0,2068	0,21	0,2088	0,21	0,2108	0,21	0,2128	0,22
42	0,1809	0,182	0,1819	0,187	0,1834	0,177	0,185	0,18	0,1865	0,19
45	0,1602	0,163	0,161	0,155	0,1622	0,165	0,1634	0,17	0,1646	0,162
48	0,1428	0,139	0,1434	0,139	0,1443	0,141	0,1453	0,14	0,1462	0,15
51	0,1279	0,124	0,1284	0,131	0,1292	0,13	0,1299	0,126	0,1307	0,132
54	0,1152	0,111	0,1156	0,112	0,112	0,117	0,1168	0,12	0,1174	0,115

Table 3: Mean Squared Error values for proposed methods.

Method	MSE (Mean Square Error)
MLPNN	2.2164E-04
RBF	0.0068
GRNN	5.5240E-04

The relative error is calculated mathematically,

$$e_{MLPNN} = \left| \frac{E_{meas} - E_{cal(MLPNN)}}{E_{meas}} \right| \times 100 \qquad (28)$$

where, E_{meas} is measurement value of the electric field, $E_{cal(MLPNN)}$ is the value of MLPNN output.

Table 4: Electric field values obtained at different coordinates by implementing Theoretical calculation, MLPNN, RBF, GRNN methods, and measurements and corresponding relative errors for each method.

Hor. Dist. (m)	Ver. Dist. (m)	Electric Field Meas. (V/m)	Electric Field Theo. (V/m)	MLPNN Calc. (V/m)	RBF Calc. (V/m)	GRNN Calc. (V/m)	e_{theo} (%)	e_{MLPNN} (%)	e_{RBF} (%)	e_{GRNN} (%)	e_{theo}-e_{MLPNN} (%)
24	0.2	0.420	0.4323	0.4339	0.2825	0.4480	2.93	3.32	32.73	6.67	0.38
30	0.2	0.320	0.3145	0.3163	0.2289	0.3111	1.72	1.17	28.47	2.77	0.56
42	0.2	0.182	0.1809	0.1805	0.1940	0.1869	0.60	0.84	6.58	2.70	0.23
51	0.2	0.124	0.1279	0.1285	0.1450	0.1310	3.15	3.63	16.95	5.65	0.47
0	0.5	1.180	1.16	1.1914	1.2836	1.2064	1.69	0.97	8.78	2.24	2.71
24	0.5	0.450	0.4379	0.4383	0.3588	0.4480	2.69	2.61	20.27	0.44	0.09
30	0.5	0.300	0.3174	0.3184	0.2511	0.3124	5.80	6.14	16.29	4.15	0.32
48	0.5	0.139	0.1434	0.1428	0.1384	0.1398	3.17	2.77	0.40	0.57	0.39
15	1	0.742	0.7524	0.7561	0.6749	0.7770	1.40	1.90	9.05	4.71	0.49
27	1	0.365	0.3783	0.3783	0.2993	0.3561	3.64	3.64	17.99	2.43	0.00
42	1	0.177	0.1834	0.1827	0.1811	0.1835	3.62	3.24	2.30	3.67	0.37
51	1	0.130	0.1292	0.1296	0.1517	0.1311	0.62	0.32	16.67	0.85	0.30
6	1.5	1.140	1.183	1.1812	1.3493	1.2173	3.77	3.62	18.36	6.78	0.15
9	1.5	1.100	1.062	1.0621	1.1121	1.0417	3.45	3.45	1.10	5.30	0.01
24	1.5	0.440	0.4569	0.4588	0.3588	0.4480	3.84	4.28	18.46	1.82	0.42
27	1.5	0.400	0.3851	0.3863	0.3391	0.3939	3.73	3.43	15.23	1.54	0.31
36	1.5	0.246	0.2421	0.2432	0.2385	0.2441	1.59	1.16	3.05	0.77	0.43
51	1.5	0.126	0.1299	0.1305	0.1522	0.1319	3.10	3.58	20.76	4.67	0.47
54	1.5	0.120	0.1168	0.1189	0.1126	0.1157	2.67	0.91	6.16	3.56	1.81
24	2	0.464	0.4666	0.4741	0.2485	0.4480	0.56	2.17	46.45	3.45	1.60
30	2	0.321	0.332	0.3358	0.2783	0.3296	3.43	4.61	13.29	2.67	1.14
42	2	0.190	0.1865	0.1871	0.1949	0.1800	1.84	1.53	2.59	5.25	0.32
45	2	0.162	0.1646	0.1647	0.1876	0.1694	1.60	1.68	15.81	4.56	0.07
48	2	0.150	0.1462	0.1465	0.1734	0.1401	2.53	2.36	15.59	6.59	0.18

Comparison of MLPNN, RBFNN and GRNN & Measurement Results with respect to Training Dataset are found in figure 6. As it can also be seen visually from the figure, the dataset of MLPNN Algorithm matches almost perfectly with the measured data. According to the mean square error analysis, and relative errors with respect to the measured values, the best results are obtained by MLPNN Algorithm. Numerical results are shown in Table 3 & Table 4. In figure 7, electric field intensity values at different heights are denoted. These results are obtained using 3 different neural algorithm methods. To be able to make a comparison and see the accuracy precision, measured values are also denoted in these graphs. Since other two methods are allowed to

alter just one parameter and MLPNN allows to change more parameters which are neuron numbers, layer numbers, activation function types etc., the most accurate result is obtained using MLPNN algorithm.

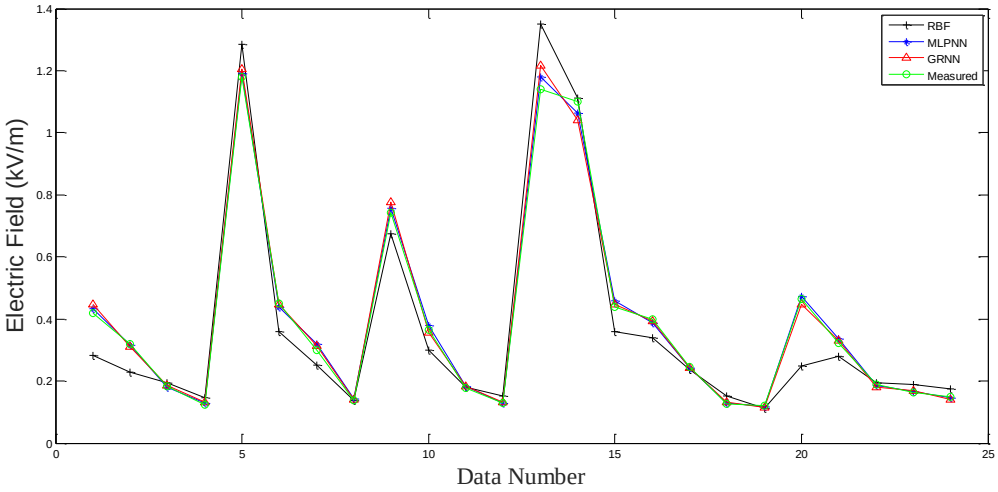

Figure 6: Comparison of MLPNN, RBFNN and GRNN & Measurement Results with respect to Training Dataset

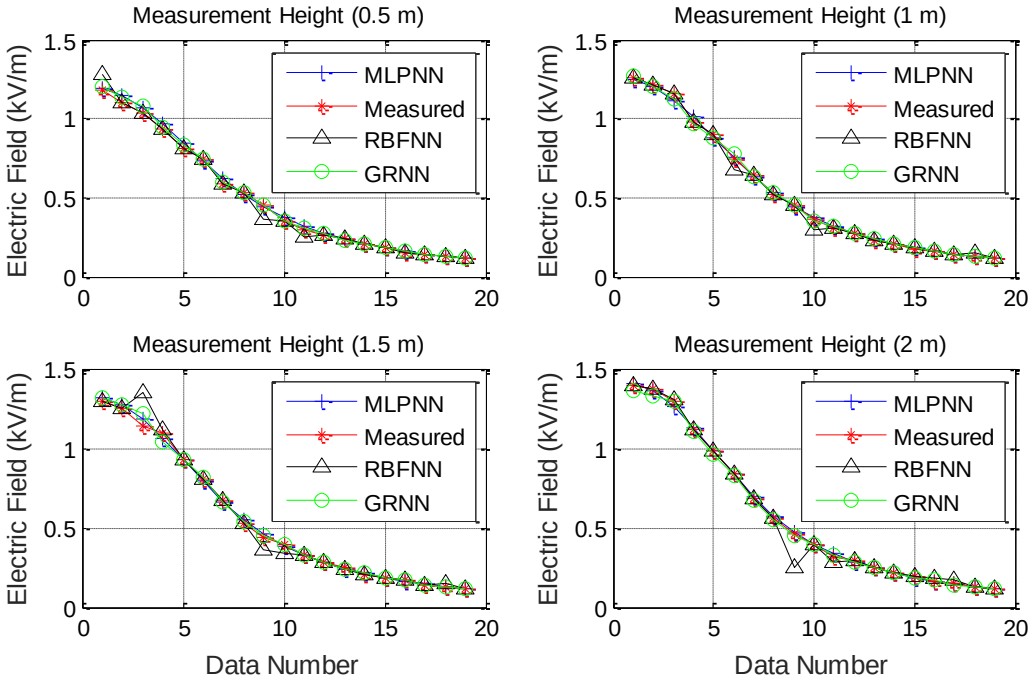

Figure 7: Predicted Electric Field Intensity Values at Different Heights Obtained with 3 different artificial neural network algorithms (MLPNN, RBFNN & GRNN Methods) and Measured Values

Figure 7 depicts the accuracy of the neural network algorithms, particularly MLPNN algorithm. Electric Field Intensity values are shown with respect to horizontal and vertical locations (see Figure 8). MLPNN results are depicted in Figure 8. As it can be seen from the Figure 8, results are obtained very precisely by using MLPNN

algorithm. Measured, theoretical and predicted neural network algorithm results are obtained in consistency. This shows the success of neural network algorithm as MLPNN. Finally, results show that the most successful neural network algorithm for calculating the electric field intensity is the MLPNN method.

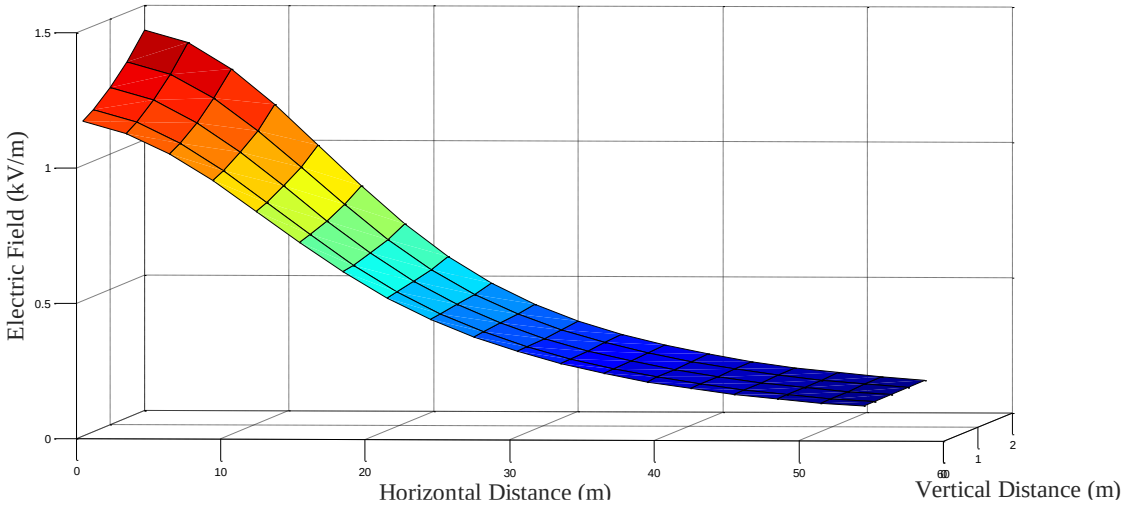

Figure 8: Electric Field Intensity Values Obtained by Applying MLPNN Algorithms at Different Heights with respect to different coordinates.

6. Conclusions

In this study, three ANN methods are compared for determination of Electric field intensity. The MLPNN method has the best accuracy results relatively. The mean square error (mse) of MLPNN algorithm is obtained as 2.2164x10-4. On the other hand, RBFNN algorithm has 0.0068 mse and GRNN has 5.5240x10-4 mse. Furthermore, maximal absolute errors of neural network methods are 6.17 % for MLPNN, 46.45% for RBFNN and 6.78% for GRNN algorithms with respect to the measurement database. As a result, the RBFNN is not sufficiently good for determination of the electric field intensity. As it is seen from the results of numerical analysis, MLPNN algorithm is the best method for calculation of electric field intensity.

The prediction of electric field intensity can be implemented with very low error by the Neural Network Algorithms, especially MLPNN method by defining the line voltage level and the physical properties of the line.

Results of the study indicate that Neural Network Algorithms particularly MLPNN can be used as a complementary tool with the conventional methods for the prediction of electric field intensity around the power transmission lines for the study of bio-electromagnetic, occupational health and safety, and electromagnetic risk analysis. To be able to keep the general public and occupational exposure under control, electromagnetic analysis of power transmission lines should be implemented daily at existing and new electric power line project designs.

Acknowledgements

The research is supported by the Research Project Department of Akdeniz University, Antalya, Turkey.

References

[1] A. Dennis, et al., "Epidemiological studies of exposures to electromagnetic fields: II. Cancer," Journal of Radiological Protection 11, 13–25, 1991.

[2] J.A. Dennis, et al., "Epidemiological studies of exposures to electromagnetic fields: I. General health and birth outcome," Journal of Radiological Protection 11, 3–12, 1991.

[3] J.W. Stather, "Epidemiological studies concerned with exposure to extremely low frequency electromagnetic fields and the risk of cancer," Radiation Protection Dosimetry 72, 291–303, 1997.

[4] J.D. Sahl, M.A. Kelsh, S. Greenland, "Cohort and nested case–control studies of hematopoietic cancers and brain cancer among electric utility workers, "Epidemiology 4 (1993) 104–114.

[5] G. Draper, et al., "Childhood cancer in relation to distance from high voltage power lines in England and Wales: a case–control study," British Medical Journal 330, 1290, 2005.

[6] J.G. Gurney, et al., "Childhood cancer occurrence in relation to power line configurations: a study of potential selection bias in case–control studies," Epidemiology 6 (1995) 31–35.

[7] S. Ozen, "Low-frequency transient electric and magnetic fields coupling to child body," Radiat Prot Dosim 128(1), 62–67, 2008.

[8] A. Albohm, et al., "Review of the epidemiologic literature on EMF and health, Environmental Health Perspectives," 109 (December 2001) pS6.

[9] J. Michaelis, J.H. Olsen, T. Tynes, P.K. Verkasalo, "A pooled analysis of magnetic fields and childhood leukemia," British Journal of Cancer 83 (5), 692–698, 2000.

[10] J.F. Deford, O.P. Gandhi, "Impedance method to calculate currents induced in biological bodies exposed to quasi-static electromagnetic fields," IEEE Trans. Electromag. Compat. Pp.168-173. Ec-27(3) (1985).

[11] M.A. Abd-Allah, Sh.A. Mahmoud, H.I Anis, "Interaction of environmental ELF electromagnetic fields with living bodies, Electric Machines And Power Systems," Vol. 28, Taylor &Francis, 301-312. 2000.

[12] MP Coleman et al., "Leukemia and residence near electrical transmission lines: a case control study," Br J Cancer. 60 (1989) Pp.793-8.

[13] Niehs, "Report on health effects from exposure to power – line frequency electric and magnetic field,"

Reported In Response To The 1992, Energy Policy Act (Pl 102-486, Section 2118).

[14] D. Noble, A. McKinlay, M. Repacholi, “Effects of static magnetic fields relevant to human health”, Eds. Progress in Biophysics and Molecular Biology, vol. 87, nos. 2-3, 171-372, February-April, 2005.

[15] IARC Monographs on the evaluation of carcinogenic risks to humans (2002), Non-ionizing radiation, Part 1: Static and extremely low-frequency (ELF) electric and magnetic fields. Lyon: International Agency for Research on Cancer, Monograph, vol. 80.

[16] Li D-K, Odoull R, Wi S, Janevic T, Golditch I, Bracken TD, Senior R, Rankin R, Iriye R., “A population-based perspective cohort study of personal exposure to magnetic fields during pregnancy and the risk of miscarriage,” Epidemiology 2002; 13:9 –20.

[17] A. Ahlbom, “Neurodegenerative diseases, suicide and depressive symptoms in relation to emf,” Bioelectromagnetics Suppl, 2001;5, S132 –S143.

[18] S. Ozen, E. G Ogel, S.Helhel, “Residential Area Medium Voltage Power Lines; Public Health, and Electric and Magnetic Field Levels,” Gazi University Journal of Science, 26(4): 573-578 (2013)

[19] DE Rumelhart, GE Hinton, RJ. Williams, “Learning representations by back propagating errors,” Nature 1986; 323:533–6.

[20] M. Hagan and M. Menhaj, "Training feedforwards networks with the Marquardt algorithm, " IEEE Transactions on Neural Networks, vol. 5 , no. 6, pp. 989-993, 1994.

[21] D. Specht, “A general regression neural network”, Neural Networks, IEEE Transactions, vol. 2, no. 6, pp. 568-576, 1991.

[22] L.V. Fausett, "Fundamentals of Neural Networks Architectures, Algorithms, and Applications," Prentice-Hall, 1994.

[23] C. Bishop,, “Improving the generalization properties of radial basis function neural networks. Neural Computation,” 3:579AS-588, 1991.

[24] S. Bilgin, O. H. Çolak, O.v Polat, E. Koklukaya, “Determination of Sympathovagal Balance in Ventricular Tachyarrhythmia Patients with Implanted Cardioverter Defibrillators Using Wavelet Transform and MLPNN,” Digital Signal Processing, Volume 19, Issue 2, 330-339, 2009.

[25] S. Ozen, S. Helhel, and H. F. Carlak, “Occupational Exposure Assessment of Power Frequency Magnetic Field in 154/31.5kV Electric Power Substation in Turkey,” PIERS Proceedings, 2015, pp. 1440-1443

[26] N. Il, S. Ozen, M. Cakir, and H. F. Carlak, “Shielding and Mitigations of the Magnetic Fields Generated by the Underground Power Cables,” PIERS Proceedings, 2015, pp. 1436-1439

[27] ICNIRP - International Commission on Non-Ionizing Radiation Protection. Exposure to static and low frequency electromagnetic fields, biological effects and health consequences (0-100 kHz). Bernhardt JH et al., eds. Oberschleissheim, International Commission on Non-ionizing Radiation Protection, 2003 (ICNIRP 13/2003).